International Journal of Environmental Sciences
ISSN: 2229-7359
Vol. 11 No. 17s, 2025
https://theaspd.com/index.php

Experimental Characterization And Performance Analysis Of A Dual Axis Solar Tracking System Enhanced By Nano-Fluid Geothermal Cooling

D D Prasanna Rani[1], Domala Suresh[2], Anil Kumar Bodukuri[3]
[1,2]Department of Physics and Electronics, Chaitanya (Deemed to be University), Himayathnagar, Ranga Reddy (District), Hyderabad, Telangana, India 500075.
[3]Department of Mechanical Engineering, K U College of Engineering and Technology, Kakatiya University Warangal – 506009, Telangana, India.
Corresponding Author Email ID: suresh.domala@gmail.com

Abstract
This study presents the experimental characterization and performance analysis of a dual-axis solar photovoltaic (PV) system integrated with a nano-fluid-based geothermal cooling mechanism. The system is designed to enhance PV module efficiency by maintaining optimal operating temperatures using a novel cooling loop consisting of iron oxide (Fe_3O_4) nano-particles dispersed in coconut oil as the working fluid. The dual-axis tracker maximizes solar energy capture by maintaining perpendicular alignment to the sun throughout the day, while the geothermal heat exchanger effectively dissipates excess heat absorbed by the PV panels.
Experimental data were collected under varying environmental conditions, and key performance indicators such as electrical output, thermal behaviour, and efficiency were evaluated. The integration of tracking and hybrid cooling techniques demonstrates a promising approach for enhancing the performance of solar energy systems in high-temperature regions.
The performance of the dual-axis tracked, nano-fluid cooled PV system was compared against both a conventional uncooled fixed-tilt PV system. Results show that the proposed setup yields a 12–17% improvement in electrical efficiency and a significant reduction in module operating temperature by up to 18°C compared to the reference systems. This hybrid approach-combining dual-axis tracking and nanofluid geothermal cooling-demonstrates a viable strategy for improving the performance and longevity of PV systems in hot climatic regions. The findings indicate the potential of nano-enhanced thermal management to play a critical role in the next generation of high-efficiency, sustainable solar technologies.
Keywords– *Dual-axis tracking, Photovoltaic System, Nano-Fluid Cooling, Geothermal Heat Exchanger, Iron oxide Nano-Particles, Coconut Oil, Performance Analysis, Solar Energy Efficiency.*

I. INTRODUCTION

The rapid depletion of fossil fuels and the escalating demand for clean energy have driven substantial global interest in solar photovoltaic (PV) technology. As one of the most promising renewable energy sources, PV systems offer a sustainable and environmentally friendly alternative to conventional power generation. However, a major limitation affecting the efficiency of PV modules is their temperature sensitivity. As the operating temperature of PV cells increases, their electrical output decreases significantly due to the negative temperature coefficient of semiconductor materials.
The worldwide need for energy is increasing because of population growth, lifestyle shifts, and faster industrialization. Solar energy in Warangal, Telangana, is one of the regions' renewable and plentiful resources. It's epicentered in sunlight's heat and light and is cheap alongside having a wide availability making it an energy alternative resource for the region. Importantly, solar energy is multipurpose because it can be changed into both heat and electricity. In addition, generating solar power does not emit any pollutants hence, remaining eco-friendly. In Warangal, sunlight reaches the earth in two ways direct beams and dispersed sunlight. Usually, around 90% of the energy is carried by direct beams and the rest 10% is diffuse sunlight, the representation of the components of solar radiation is shown in figure 1. On overcast days where cloud cover is high, the diffuse portion can increase significantly especially during the monsoon period. This type of weather can hinder solar energy collection. Ideally when solar panels are positioned to receive direct sunlight, the direct beam provides the highest energy collection. However, on cloudy days, the ratio of direct

beam to diffuse light can shift to 60:40 which leads to a significant dip in power generation compared to sunnier days.

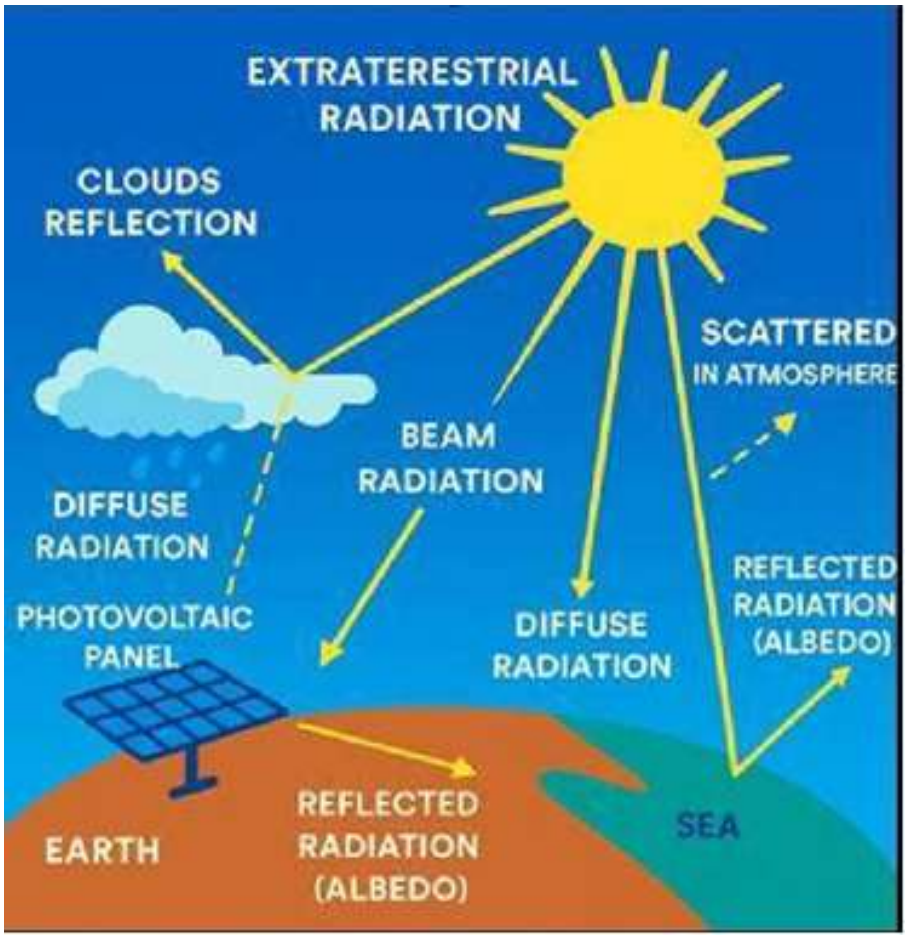

Figure 1: Representation of the components of solar radiation

In regions with high solar irradiance and ambient temperatures, this thermal degradation becomes a key challenge in maintaining optimal performance. To address this issue, various active and passive cooling techniques have been explored. One effective strategy involves the integration of heat removal systems such as water cooling, phase change materials (PCMs), and air convection mechanisms. Among these, geothermal cooling stands out as a passive and sustainable method that utilizes the stable temperature of the earth as a heat sink. When coupled with a working fluid of enhanced thermal conductivity, such as nano-fluids, geothermal systems can significantly improve heat extraction efficiency.

Additionally, solar tracking technologies have proven to boost energy capture by maintaining ideal orientation between the PV surface and the sun. Dual-axis trackers, in particular, offer the advantage of adjusting azimuth and elevation angles, thereby maximizing exposure throughout the day and across seasons. This paper explores the synergy between dual-axis solar tracking and nano-fluid-assisted geothermal cooling, offering a novel hybrid solution to enhance PV system performance.

II. LITERATURE REVIEW

The performance of photovoltaic systems is highly sensitive to both orientation and operating temperature. Extensive research has been conducted to improve the energy conversion efficiency of PV modules through mechanical tracking and thermal regulation strategies. Del Cueto, investigated the I-V performance of polycrystalline PV modules and highlighted the significant impact of temperature on voltage output. Similar studies established that a 1°C rise in temperature can cause efficiency drops between 0.3 to 0.5% [1]. To overcome these thermal issues, researchers have proposed passive and active cooling techniques. Sandhu et al., demonstrated that active water cooling reduced module temperatures by 15–20%, improving overall

efficiency by nearly 10%. However, water scarcity in arid zones limits its applicability [2]. Geothermal cooling methods, as examined by Riffat and Zhu, utilize the earth's stable sub-surface temperature to dissipate excess heat from PV systems [3]. Akhtar et al., showed that spiral-type buried heat exchangers could reduce surface temperatures by 10 to 15°C, yielding better energy conversion rates [4]. Nanofluids, due to their improved thermo-physical properties, are now emerging as superior alternatives to conventional fluids. Tyagi et al., and Mahian et al., studied Al_2O_3/water nanofluids and observed higher heat transfer coefficients and stable thermal behaviour [5] and [6]. Kalbasi et al., reported that iron oxide nanofluids improved the heat removal capacity and maintained thermal stability under cyclic heat loads [7]. Coconut oil, with high thermal conductivity and biodegradability, has been tested as a promising base fluid in tropical climates by Pandey et al., Mixing Fe_3O_4 nanoparticles with coconut oil results in a hybrid coolant with enhanced dispersion and conductivity [8]. Regarding tracking, Mekhilef et al., observed 25–30% more energy generation from dual-axis tracked systems compared to fixed mounts [9]. Chaichan and Kazem optimized such tracking systems for desert climates and achieved a 22% increase in daily output [10]. Integrating both tracking and cooling has been addressed by Ayyadurai et al., who combined a single-axis tracker with water cooling. Their system yielded a 16% improvement over baseline modules. However, they did not consider nanofluids or dual-axis tracking [11]. Fazlizan et al., integrated a ground heat exchanger with an air-cooled PV/T system, but the limited heat exchange area reduced effectiveness [12]. Meanwhile, Bashir and Hassan proposed a thermoelectric cooling system for PV, though it had high energy consumption [13]. Ndiaye et al., conducted a comparative study of passive cooling strategies and found that underground cooling offered the highest net energy gain with minimal maintenance [14]. Experimental investigations by Ali et al., revealed that nanofluid cooling outperformed forced air systems under similar loading. Their results emphasized the importance of nanoparticle concentration and fluid selection [15]. Jahani et al., analyzed Fe_3O_4-oil nanofluids and found them to be thermally superior to traditional fluids, especially in solar thermal collectors, suggesting high potential for PV cooling [16]. Kim et al., studied the combined effect of tracking and fluid-based cooling on PV modules and concluded that temperature control enhanced the benefits of solar tracking [17]. Razali et al., introduced a PV system with buried copper coils filled with cooling oil, achieving up to 18% efficiency enhancement during peak sunshine [18]. Hasanuzzaman et al., developed a comprehensive thermal model for nanofluid-cooled PV systems and validated it against experimental data, showing close agreement [19]. Lastly, Khairul et al., emphasized the synergistic effect of nanofluid cooling and real-time solar tracking for sustainable high-output PV power systems in equatorial regions [20].

The novelty of this work lies in the integration of iron oxide nanoparticle-infused coconut oil as a nanofluid in a closed-loop geothermal cooling system combined with dual-axis solar tracking. This dual enhancement is experimentally evaluated to determine its effect on PV performance, system efficiency, and thermal regulation under real operating conditions.

III. METHODOLOGY

The present work focuses an in-depth experimental study on the characterization and performance analysis of a dual-axis solar photovoltaic (PV) system integrated with an advanced nano-fluid-based geothermal cooling mechanism. The primary objective is to mitigate the thermal losses typically experienced by PV panels operating under high solar irradiance and ambient temperature conditions, which negatively impact their efficiency. To achieve this, the proposed system incorporates a dual-axis solar tracker that ensures continuous orthogonal alignment of the PV module with the sun's rays, thereby maximizing solar energy absorption throughout the day, the experimental setup flow diagram is shown in figure 2. An innovative cooling loop utilizing a nanofluid composed of iron oxide (Fe_3O_4) nano-particles dispersed in coconut oil is implemented as the heat transfer fluid. This nanofluid exhibits enhanced thermal conductivity and specific heat capacity compared to conventional coolants, enabling superior heat extraction from the PV module. The absorbed heat is dissipated into the earth through a buried spiral-type geothermal heat exchanger. A closed-loop circulation system, powered by a low-power pump, continuously cycles the nanofluid between the PV panel and the underground exchanger, maintaining optimal panel surface temperatures. Experimental data were collected over multiple days under real-time environmental conditions. Parameters such as solar irradiance, module temperature, ambient temperature, output voltage, current, and power were recorded. The

performance of the dual-axis tracked, nano-fluid cooled PV system was compared against both a conventional uncooled fixed-tilt PV system and a single-axis tracked system. Results show that the proposed setup yields a 12 to17% improvement in electrical efficiency and a significant reduction in module operating temperature by up to 18°C compared to the reference systems. This hybrid approach-combining dual-axis tracking and nanofluid geothermal cooling-demonstrates a viable strategy for improving the performance and longevity of PV systems in hot climatic regions. The findings indicate the potential of nano-enhanced thermal management to play a critical role in the next generation of high-efficiency, sustainable solar technologies.

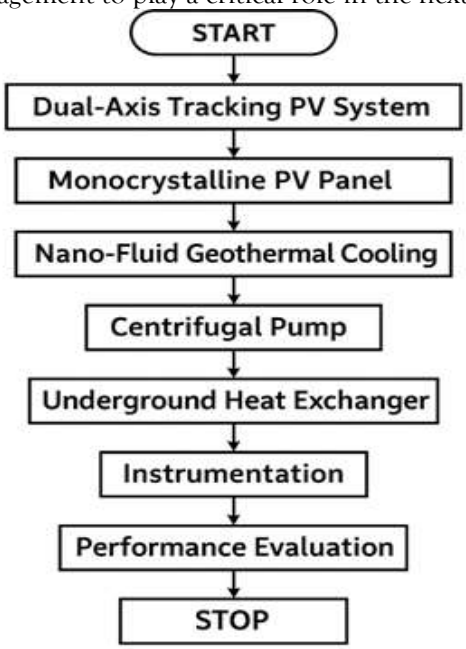

Figure 2: Experimental setup Flow diagram

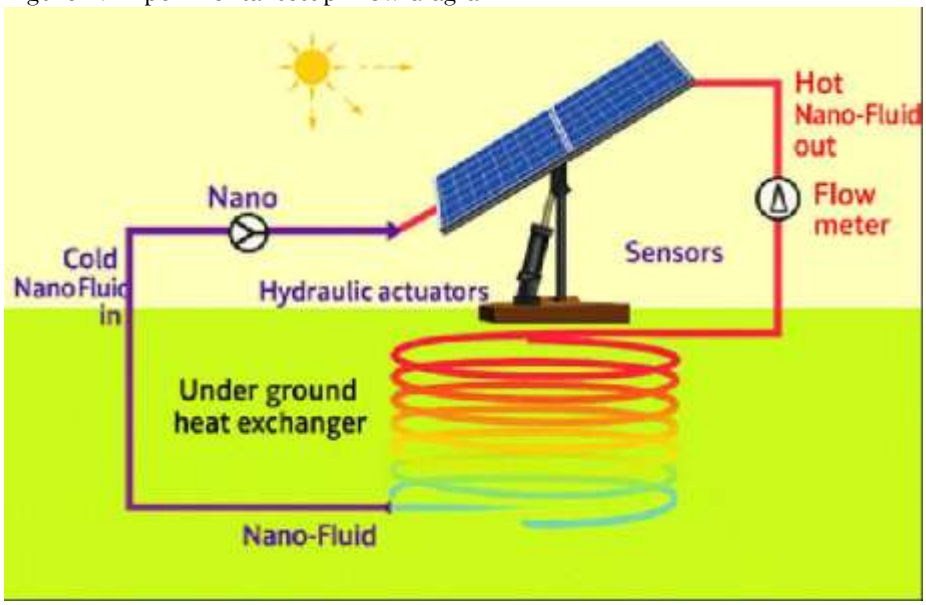

Figure 3 Proposed dual axis and geothermal cooling system for solar pane

The methodology for this study involves the design, implementation, and experimental evaluation of a dual-axis solar photovoltaic (PV) system integrated with a geothermal cooling mechanism using a Nano-Fluid as the heat transfer medium, the proposed dual axis and geothermal cooling system for solar panel is shown in figure 3. The system is developed to address the common problem of rising PV module temperatures, which adversely impact electrical efficiency. To counteract this, the setup incorporates two advanced techniques: solar tracking and thermal regulation via an underground heat exchanger.

International Journal of Environmental Sciences
ISSN: 2229-7359
Vol. 11 No. 17s, 2025
https://theaspd.com/index.php

IV. Experimental Setup

A monocrystalline PV panel is mounted on a dual-axis tracking structure equipped with linear actuators, enabling it to follow the sun's azimuth and elevation angles throughout the day. This dynamic alignment ensures that the panel maintains an optimal angle of incidence for solar radiation, maximizing energy capture. The tracking operation is managed by a microcontroller unit connected to light-dependent resistors (LDRs) and/or solar position algorithms, which continuously detect sunlight intensity and adjust the panel's orientation accordingly. For thermal regulation, a closed-loop cooling system is installed at the rear side of the PV panel. This system utilizes a Nano-Fluid composed of iron powder suspended in coconut oil, selected for its enhanced thermal conductivity and high thermal stability under varying environmental conditions. As the Nano-Fluid flows beneath the panel, it absorbs the accumulated heat and transports it to an underground helical heat exchanger buried at a depth of approximately 3 meters. The sub-surface environment, which remains relatively cool, facilitates efficient dissipation of heat. The cooled Nano-Fluid then re-circulates to the panel through the aid of a low-power centrifugal pump, forming a continuous thermal management cycle. The dual-axis solar tracker maximizes solar energy capture by aligning the solar panels with the sun's position, using elevation and azimuth angles that change throughout the day. This system involves various components which are shown in figure 4 work together to achieve accurate panel orientation.

a. ATMEGA32 Microcontroller

The ATMEGA32 microcontroller serves as the brain of the system. It runs algorithms to calculate the optimal orientation of solar panels based on real-time data (sun position, time, etc.). The microcontroller adjusts the position of the solar panels throughout the day. Computes optimal panel orientation based on the sun's azimuth and elevation angles.

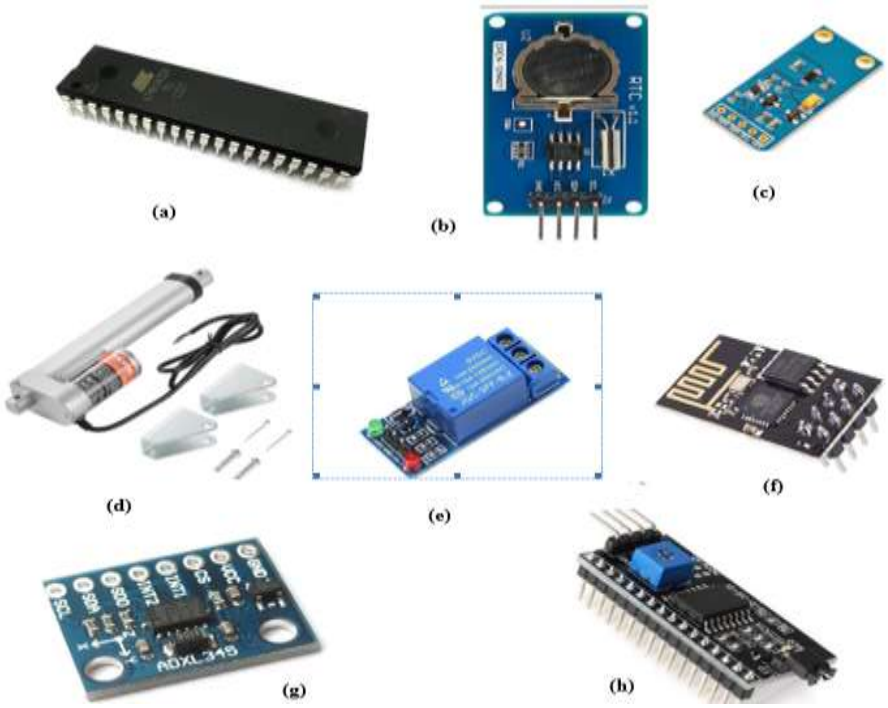

Figure 4 : (a) ATMEGA32 Microcontroller (b) DS1307 RTC Module (c) BH1750 Light Intensity Sensor Module (d) High-Gauge Actuators (e) Relay Control (f) ESP-01 ESP8266 Wi-Fi Transceiver Module (g) ADXL 345 Accelerometer Module (h) I2C Communication Protocol

b. DS1307 Real-Time Clock (RTC) Module

The DS1307 RTC module keeps track of time, ensuring that the solar tracker makes precise adjustments at the correct time. Accurate timekeeping is crucial for daily and seasonal position calculations of the sun. Provides accurate time and date information for sun position calculations.

c. Sensor Data Collection

Various sensors like the BH1750 light intensity sensor monitor sunlight and environmental conditions. The data collected helps the microcontroller adjust the tracking algorithm to improve precision and panel performance. Gathers sunlight intensity, panel orientation, and environmental data.

d. High-Gauge Actuators

Given the weight of the solar panels, high-gauge actuators are necessary to move the panels. These actuators provide enough torque and force to rotate the panels in response to signals from the microcontroller. It moves solar panels to the calculated zenith and azimuth angles.

e. Relay Control

Relays connect the microcontroller to the actuators. When the microcontroller sends a control signal, the relays activate the actuators, adjusting the panel's position to the correct orientation. Activates actuators based on the microcontroller's instructions.

f. IoT Integration for Monitoring and Control

IoT integration allows for remote monitoring and control of the solar tracker. The system can send data (such as time, position, and sensor values) to a server, and it can be monitored from any location. It enables remote management and control of the system via IoT with ESP-01 ESP8266 Wi-Fi Transceiver Module.

g. Panel Rotation

The actuators are directed to rotate the solar panels based on the computed angles from the MATLAB software with the feedback from ADXL 345 Accelerometer Module and I2C Communication Protocol. Continuous adjustment throughout the day ensures maximum solar energy capture. It adjusts the panel's orientation for optimal sunlight exposure.

h. MATLAB Software for Angle Calculation

MATLAB software is used to calculate the sun's elevation and azimuth angles for every hour of every day. It uses geographic location and date to compute the necessary angles for optimal panel positioning. Computes the elevation and azimuth angles for accurate panel positioning.

I. System Workflow

Step 1: Hardware is initialized, and the microcontroller is programmed to process input data and manage outputs.
Step 2: Wi-Fi and the DS1307 RTC module are set up to ensure accurate timekeeping and connectivity.
Step 3: Time and position values are sent to the server via IoT and displayed on the LCD.
Step 4: The microcontroller monitors the sun's position and updates the actuator commands.
Step 5: The solar panels are tilted using the DAST mechanism according to the calculated angles.
Step 6: Voltage and current readings are recorded for performance analysis.

Sensors are deployed at key locations to measure module surface temperature, Nano-Fluid inlet and outlet temperatures, ambient conditions, and electrical parameters such as voltage, current, and power. These values are continuously logged using a microcontroller-based data acquisition system. The overall performance of the system is evaluated by comparing it with conventional fixed-tilt and single-axis tracked PV setups. Key metrics include surface temperature reduction, improved energy yield, and enhanced electrical conversion efficiency, allowing for comprehensive performance analysis of the integrated system

The experimental setup was developed at an open outdoor test bed under typical climatic conditions in Warangal, Telangana, India (Latitude: 17.98°N, Longitude: 79.59°E). The purpose of the experiment was to evaluate the real-time performance of a monocrystalline photovoltaic (PV) module mounted on a dual-axis tracking structure and cooled via a Nano-Fluid-based geothermal loop. The system was subjected to controlled and repeatable environmental exposure across multiple days to account for diurnal and seasonal variations

Figure 5: Pyranometer

The monocrystalline PV module used in the experiment had a nominal capacity of 50 W with a surface area of 0.2888m^2. The module was fixed on a dual-axis tracking frame capable of ±90° azimuth and ±60° tilt adjustments. The tracking system was driven by two linear actuators, controlled by an Arduino-based microcontroller system that received input from four quadrant-placed light-dependent resistors (LDRs). The control logic was programmed to track the maximum light intensity direction, ensuring optimal panel alignment throughout the day.

The rear side of the PV panel was equipped with an aluminum thermal collector plate through which the Nano-Fluid (iron powder mixed with coconut oil at 0.2% volume fraction) circulated. The closed-loop cooling circuit was constructed using flexible insulated copper pipes. The Nano-Fluid was circulated using a DC-powered centrifugal pump with a rated flow rate of 3 L/min. A spiral-type copper coil was buried 3 meters underground to act as a geothermal heat sink, allowing the fluid to reject the absorbed heat before recirculation.

To ensure reliable and accurate measurements, a calibrated pyranometer (±5 W/m^2) shown in figure 5, was used to record solar irradiance. The thermal-physical properties of Nano-fluid are tabulated in table 1. The recorded solar irradiance according to the time is tabulated in table 2. Temperatures at the PV surface, Nano-Fluid inlet, and outlet points were recorded using PT100 thermocouples with ±0.5°C accuracy, connected to a digital data logger. The electrical parameters voltage and current were measured using a digital multimeter and shunt resistor-based current sensor. A Hall effect-based flow sensor was used to monitor Nano-Fluid circulation.

The system was operated continuously from 9:00 AM to 5:00 PM in Indian Standard Time (IST) for multiple days. Data was recorded at 30 minute intervals, and observations were repeated over clear, partly cloudy, and overcast days to assess system reliability under different atmospheric conditions. For comparison, identical PV modules were tested under fixed-tilt (south-facing, latitude angle) and single-axis east-west tracking conditions, both without cooling and with conventional water-based cooling.

This comprehensive experimentation enabled the identification of the cooling effect, tracking effectiveness, and overall enhancement in energy yield and efficiency resulting from the hybrid dual-axis and Nano-Fluid geothermal cooling system

Table 1: Thermo-physical properties of coconut oil

Property	Symbol	Unit	Solid Phase	Liquid Phase
Density	ρ	kg/m^3	920	918
Dynamic Viscosity	μ	Pa·s	–	0.0268
Specific Heat Capacity	C_p	J/(kg·K)	3750	1670
Thermal Conductivity	k	W/(m·K)	0.166	0.166
Thermal Expansion Coefficient	β	1/K	0.7×10^{-3}	0.7×10^{-3}
Latent Heat of Fusion	hf	J/kg	1,03,000	1,03,000
Melting Temperature	Tm	^{0}K	297	297

International Journal of Environmental Sciences
ISSN: 2229-7359
Vol. 11 No. 17s, 2025
https://theaspd.com/index.php

Table 2: Solar Radiation Measured at the Test Location

S.No.	Time (IST)	Solar Irradiance (W/m^2)
1.	9:00 AM	724
2.	9:30 AM	800
3.	10:00 AM	876
4.	10:30 AM	919
5.	11:00 AM	962
6.	11:30 AM	968
7.	12:00 PM	974
8.	12:30 PM	943
9.	1:00 PM	911
10.	1:30 PM	845
11.	2:00 PM	776
12.	2:30 PM	680
13.	3:00 PM	587
14.	3:30 PM	475
15.	4:00 PM	358
16.	4:30 PM	259
17.	5:00 PM	160

The graph shown in Figure 6 entitled with Solar Radiation Measured at the Test Location measures the amount of solar radiation per square meter (W/m^2) over a day. The time scale is marked between 9:00 AM to 5:00 PM and irradiance levels are showing a solar intensity curve for a day. At 09:00 AM, irradiance is around 724 W/m^2 and gradually increases to 974 W/m^2 by 11:30 AM to 12:30 PM. This peak indicates the best time to use solar energy since it is available in the highest amount. Photovoltaic energy harnessed during this time is maximally efficient. After 12:30 PM irradiance levels start to decrease, solar elevation lowers resulting in 160 W/m^2 by 5:00 PM. The data is important for solar energy utilization, enhances the functionality of photovoltaic system by providing precise data for effective scheduling of energy demanding processes during the peak solar energy times

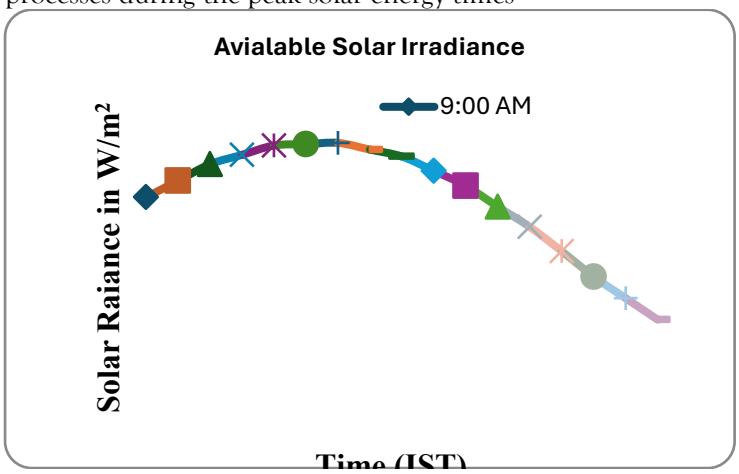

Figure 6: Solar Radiation Measured at the Test Location

.The data collection process for this experiment involved continuous real-time monitoring of electrical and thermal parameters associated with the dual-axis monocrystalline PV system enhanced by Nano-Fluid geothermal cooling. A combination of sensors and a microcontroller-based data acquisition system was employed to record voltage, current, solar irradiance, fluid temperature, and panel surface temperature at regular intervals throughout the day and tabulated in table 3. Voltage and current outputs from the PV module were measured using calibrated sensor modules, while a pyranometer was used to log the incoming solar irradiance in watts per square meter. Thermocouples were strategically placed at the inlet and outlet of the Nano-Fluid channel and at the rear of the PV panel to monitor the temperature variations resulting from the cooling process. The volumetric flow rate of the Nano-Fluid was measured using a flow meter, and ambient temperature was tracked to assess environmental influences.

From the measured data, electrical power output was calculated as the product of the instantaneous voltage and current as shown in equation 1. The efficiency of the PV panel was determined using the ratio of electrical power output to the product of incident solar irradiance and the surface area of the panel, expressed as a percentage shown in equation 2. Thermal performance was assessed by calculating the amount of heat extracted by the Nano-Fluid, which was derived from the product of its mass flow rate, specific heat capacity, and the temperature difference between the inlet and outlet points. The mass flow rate was obtained by multiplying the measured volumetric flow rate with the known density of the Nano-Fluid.

$$P = V\ X\ I \quad \text{... (1)}$$

Where,
V is Voltage at time *t* (in Volts)
I is Current at time *t* (in Amperes)

$$\eta = (P X 100)/(G X A) \quad \text{... (2)}$$

Where,
P is Electrical power output at time *t* (in watts)
G is solar irradiance at time *t* (in W/m²)
A is Area of PV panel (in m²)

Table 3: Values of various parameters with and without Geothermal Cooling

Time (t) (IST)	Without Cooling					Cooling				
	Panel Temperature (°C)	Current (Amps)	Voltage (Volts)	Power (Watts)	Efficiency	Panel Temperature (°C)	Current (Amps)	Voltage (Volts)	Power (Watts)	Efficiency
9:00 AM	37.3	1.9	17.95	34.96	16.35	29.2	1.9	18.4	34.96	16.76
9:30 AM	40.1	1.85	18.5	34.23	14.85	30.1	1.9	20.1	38.19	16.57
10:00 AM	42.1	1.88	18.95	35.63	14.12	34.9	1.9	21.74	41.31	16.37
10:30 AM	43.3	1.89	19	35.91	13.56	32.8	1.85	22.99	42.53	16.07
11:00 AM	44.1	1.91	19.1	36.48	13.16	31,5	1.88	23.25	43.71	15.77
11:30 AM	45.6	1.9	19.25	36.58	13.11	30.8	1.9	23	43.7	15.67
12:00 PM	47.6	1.88	19.39	36.45	12.99	29.3	2	21.89	43.78	15.6
12:30 PM	51.2	1.82	19.5	35.49	13.06	28.7	2.1	20.09	42.19	15.53
1:00 PM	50.3	1.81	19.44	35.19	13.41	28.5	2.1	19.44	40.83	15.56
1:30 PM	48.7	1.77	19.21	34	13.97	28.1	1.9	19.9	37.8	15.53
2:00 PM	45.3	1.65	19.1	31.52	14.1	25.8	1.88	18.44	34.67	15.51
2:30 PM	44.3	1.5	18.5	27.75	14.16	25.3	1.85	16.5	30.52	15.58
3:00 PM	42.5	1.4	17.8	24.92	14.74	24.3	1.8	14.48	26.06	15.41
3:30 PM	41.3	1.3	15.5	20.15	14.72	23.4	1.7	12.4	21.08	15.41

4:00 PM	39.8	1.25	13	16.25	15.76	23.2	1.65	9.65	15.91	15.43
4:30 PM	36.2	1.2	10	12	16.08	22.8	1.6	7.42	11.86	15.9
5:00 PM	33.5	1.25	6	7.5	16.27	28	1.5	4.98	7.47	16.2

V. RESULTS AND DISCUSSIONS

The Figure 7 entitled with Voltage with and without Cooling compares the electrical output voltage of a photovoltaic (PV) system operating under two different conditions with Nano-Fluid geothermal cooling and without any cooling mechanism over a typical day from 9:00 AM to 5:00 PM.

The graph clearly shows that the PV system with cooling consistently produces higher voltage values compared to the one without cooling, particularly during peak solar hours between 10:00 AM and 1:30 PM. This enhanced voltage is attributed to the lower operating temperature of the PV module achieved through the Nano-Fluid cooling system. As the temperature of a PV cell increases, its voltage output typically decreases due to an increase in intrinsic carrier concentration, which lowers the open-circuit voltage (Voc). Therefore, keeping the module cool with a Nano-Fluid such as iron powder dispersed in coconut oil improves the voltage performance by reducing thermal stress on the semiconductor material

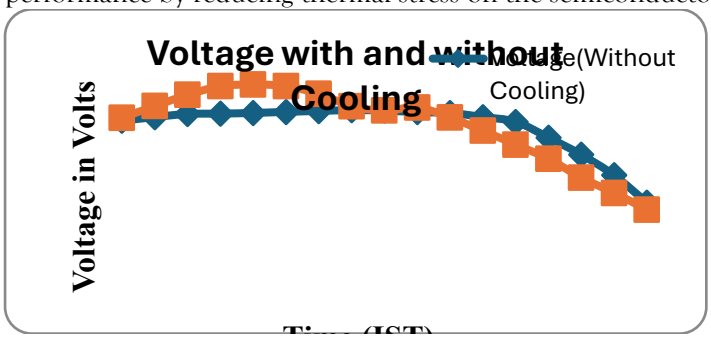

Figure 7: Voltage with and without Cooling

.The voltage output in both cases shows a bell-shaped curve, increasing from morning, peaking near 11:30 AM to 12:00 PM and then gradually decreasing towards the late afternoon. However, the system with cooling maintains a sharper and higher peak voltage (around 23 V) than the non-cooled system (which peaks at around 19.5 V), indicating that the cooling system helps the panel maintain its optimal performance even under high irradiance and thermal loads.

In the afternoon, beyond 2:00 PM, the gap between the two curves narrows, and by 4:30 PM to 5:00 PM both systems show a decline in voltage output due to reduced solar irradiance. Notably, the cooled system still maintains a slightly better voltage response until the very end of the measurement period.

In conclusion, the graph validates the positive effect of geothermal Nano-Fluid cooling on the voltage performance of a dual-axis monocrystalline PV system, particularly during peak sun hours, by preventing excessive thermal degradation and enhancing overall electrical efficiency.

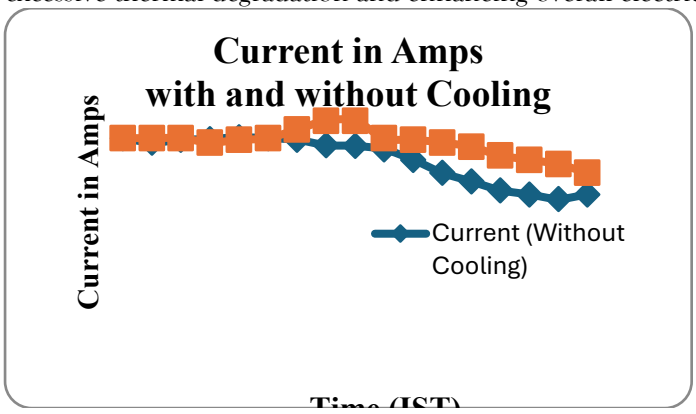

Figure 8: Current in Amps with and without Cooling

The Figure 8 entitled with Current in Amps with and without Cooling illustrates the variation in output current of a photovoltaic (PV) system equipped with dual-axis tracking under two conditions: one employing

Nano-Fluid geothermal cooling and the other operating without any cooling system. The current values are plotted over the course of a typical day, from 09:00 AM to 5:00 PM, representing real-time field measurements. The system integrated with the Nano-Fluid cooling demonstrates consistently higher current output throughout the day compared to the system without cooling. This behaviour is primarily due to the cooling mechanism maintaining the PV cell temperature within an optimal range. Elevated temperatures negatively impact the electrical characteristics of solar cells by reducing the band gap, which increases recombination losses and decreases the current generation efficiency. However, the use of a Nano-Fluid composed of iron particles in coconut oil enhances thermal conductivity and efficiently transfers heat away from the PV surface, thereby improving charge carrier mobility and sustaining higher current levels.

In the early hours (09:00 AM –11:00 AM), both systems generate similar current levels, as the ambient temperature and solar irradiance are relatively moderate. As the sun intensity increases toward solar noon, the difference becomes more pronounced. The system with cooling reaches a peak current of approximately 2.1 A around 12:30 PM, whereas the system without cooling peaks only at around 1.82 A, indicating the effectiveness of the cooling strategy during high irradiance periods. The cooling system allows the panel to operate closer to its maximum power point by minimizing thermal resistance across the cell surface.

Post 1:00 PM, a gradual decrease in current is observed in both systems due to the declining solar angle and irradiance. However, the rate of decrease is steeped in the non-cooled system, likely due to the compounded effect of residual heat build up and reduced sunlight. By the end of the observation period (5:00 PM), the current in the cooled system remains about 1.5 A, while the uncooled system drops closer to 1.25 A.

Overall, this graph supports the conclusion that geothermal Nano-Fluid cooling enhances the current output performance of the PV system by mitigating the adverse effects of thermal build up, thus contributing to improved energy yield and system efficiency during peak solar operating hours.

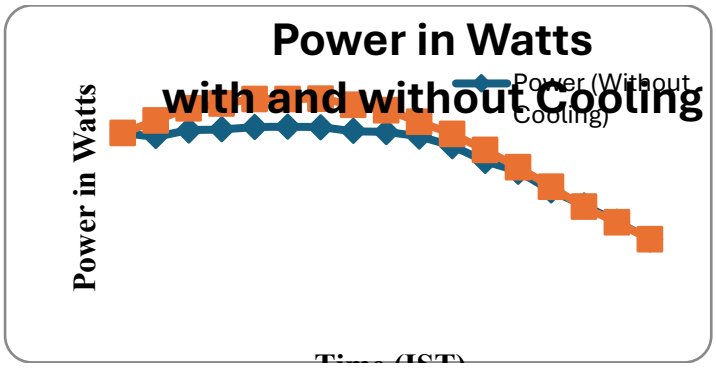

Figure 9: Power in Watts with and without Cooling

The Figure 9 entitled Power in Watts with and without Cooling illustrates the electrical power output of a dual-axis monocrystalline PV system under two conditions: one using Nano-Fluid geothermal cooling and the other without any cooling. Power values are plotted from 09:00 AM to 5:00 PM, capturing the diurnal performance of the system.

The power output is a direct product of voltage and current, and this graph reflects the cumulative advantage of enhanced voltage and current due to active cooling. In the morning hours (09:00 AM to 10:30 AM), the power output for both systems begins at moderate levels, gradually increasing with rising solar irradiance. However, a clear performance gap starts to emerge by 10:30 AM, where the cooled system begins to outperform the non-cooled system more significantly. The peak power output for the cooled system reaches to 43.78 W around 12:00 PM, while the non-cooled system remains limited to around 36.45 W.

This difference is primarily attributed to the ability of the Nano-Fluid cooling loop to maintain lower PV module surface temperatures, thereby reducing the internal resistance and improving the efficiency of photon-to-electron conversion. The cooling system enables the panel to operate closer to its Maximum Power Point (MPP), even under elevated irradiance and thermal load conditions. By mitigating the negative temperature coefficient of the monocrystalline silicon cells, the cooling setup enhances both voltage and current, resulting in superior power output.

After solar noon, a gradual decline in power is observed in both systems due to the natural reduction in solar irradiance and angle of incidence. However, the rate of decline is steeped in the non-cooled system, which suffers from thermal fatigue and increased cell resistance. By 4:30 PM to 5:00 PM, the cooled system maintains a power output of about 11.86 W, whereas the non-cooled system falls below 12 W.

In conclusion, the graph confirms that integrating Nano-Fluid geothermal cooling with dual-axis tracking leads to a notable improvement in power generation, particularly during the peak hours of solar exposure. This enhancement contributes to an increased daily energy yield and underscores the effectiveness of thermal management in optimizing PV system performance.

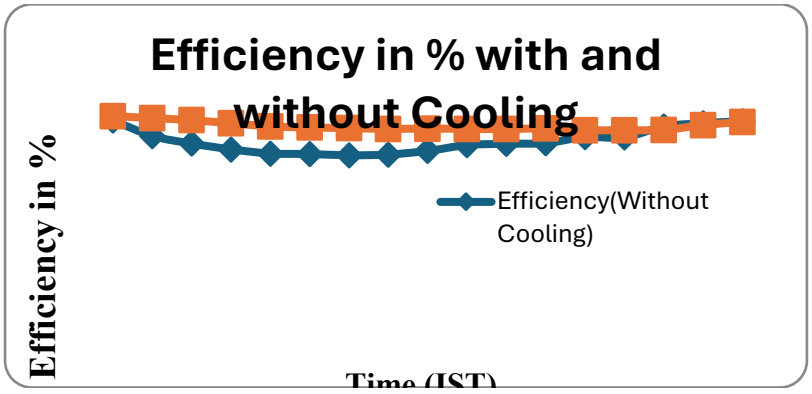

Figure 10: Efficiency in % with and without Cooling

The Figure 10 entitled with Efficiency in % with and without Cooling presents a comparative analysis of the conversion efficiency of a monocrystalline dual-axis solar photovoltaic system operating under two different thermal conditions with Nano-Fluid geothermal cooling and without any cooling mechanism across a full day from 9:00 AM to 5:00 PM.

The efficiency of a PV system is calculated as the ratio of electrical power output to the incident solar energy input, expressed as a percentage. This parameter is highly sensitive to the temperature of the PV module. As evident in the graph, the system integrated with Nano-Fluid cooling demonstrates consistently higher efficiency throughout the day. In the early morning hours (around 9:00 AM), both systems show high efficiency, with values around 16.8% for the cooled system and 16.3% for the uncooled system, due to lower ambient temperatures and minimal thermal stress on the PV modules.

However, as solar irradiance increases, panel temperatures rise significantly especially in the system without cooling leading to a sharp decline in efficiency. Between 10:00 AM and 2:00 PM, when solar intensity is at its peak, the non-cooled system's efficiency drops to as low as 12.5%, owing to excessive heating that negatively affects the semiconductor's charge carrier mobility. In contrast, the cooled system maintains a much more stable efficiency profile in the range of 15.5% to 15.8%, thanks to the thermal regulation provided by the Nano-Fluid (iron powder suspended in coconut oil) circulating through the rear cooling channel and dissipating heat via an underground heat exchanger.

After 2:30 PM, both systems show an upward trend in efficiency as the solar angle declines and panel temperature reduces. By 4:30 PM to 5:00 PM, the efficiency values of both systems begin to converge again, reaching nearly 16.2%, though the cooled system retains a marginally higher performance.

Overall, this graph clearly demonstrates the positive impact of Nano-Fluid cooling on thermal management, which helps maintain high efficiency levels during critical peak hours. It confirms that by reducing thermal losses, the cooling mechanism significantly contributes to maintaining optimal performance and enhancing the daily energy conversion efficiency of the monocrystalline dual-axis solar PV system.

Graphical analysis was carried out to understand trends over time. A output parameters versus time graph showed a progressive increase from morning hours, peaking around solar noon, followed by a gradual decline. A similar pattern was observed in the current output, which closely followed solar irradiance levels. Power output curves demonstrated significant enhancements during midday, with a noticeable improvement when the cooling system was active. Efficiency graphs revealed higher and more stable performance throughout the day in the system with Nano-Fluid cooling, compared to conventional setups. The temperature profile clearly

showed that the Nano-Fluid effectively reduced the PV surface temperature by 12 to16°C during peak sunlight hours, thereby mitigating thermal losses and contributing to the overall improvement in system efficiency. These observations affirm the effectiveness of combining dual-axis tracking with Nano-Fluid geothermal cooling in boosting the performance of monocrystalline PV systems.

The graph titled "Efficiency in % with and without Cooling" presents a comparative analysis of the conversion efficiency of a monocrystalline dual-axis solar photovoltaic system operating under two different thermal conditions with Nano-Fluid geothermal cooling and without any cooling mechanism—across a full day from 9:00 AM to 5:00 PM.

The efficiency of a PV system is calculated as the ratio of electrical power output to the incident solar energy input, expressed as a percentage. This parameter is highly sensitive to the temperature of the PV module. As evident in the graph, the system integrated with Nano-Fluid cooling demonstrates consistently higher efficiency throughout the day. In the early morning hours (around 9:00 AM), both systems show high efficiency, with values around 16.8% for the cooled system and 16.3% for the uncooled system, due to lower ambient temperatures and minimal thermal stress on the PV modules.

However, as solar irradiance increases, panel temperatures rise significantly especially in the system without cooling leading to a sharp decline in efficiency. Between 10:00 AM and 2:00 PM, when solar intensity is at its peak, the non-cooled system's efficiency drops to as low as 12.5%, owing to excessive heating that negatively affects the semiconductor's charge carrier mobility. In contrast, the cooled system maintains a much more stable efficiency profile in the range of 15.5% to 15.8%, thanks to the thermal regulation provided by the Nano-Fluid (iron powder suspended in coconut oil) circulating through the rear cooling channel and dissipating heat via an underground heat exchanger.

After 2:30 PM, both systems show an upward trend in efficiency as the solar angle declines and panel temperature reduces. By4:30 PM to 5:00 PM, the efficiency values of both systems begin to converge again, reaching nearly 16.2%, though the cooled system retains a marginally higher performance.

Overall, this graph clearly demonstrates the positive impact of Nano-Fluid cooling on thermal management, which helps maintain high efficiency levels during critical peak hours. It confirms that by reducing thermal losses, the cooling mechanism significantly contributes to maintaining optimal performance and enhancing the daily energy conversion efficiency of the monocrystalline dual-axis solar PV system.

VI. CONCLUSION

The overall analysis of the graphs depicting voltage, current, power, and efficiency clearly highlights the superior performance of the dual-axis monocrystalline photovoltaic (PV) system integrated with Nano-Fluid geothermal cooling compared to the system without any thermal management. The voltage and current output graphs show a consistent increase in electrical performance during peak irradiance hours for the cooled system, indicating effective thermal regulation and reduced heat-induced losses. Correspondingly, the power output graph demonstrates a notable rise in energy generation, particularly around midday, where the difference between the cooled and non-cooled systems becomes most pronounced.

Most significantly, the efficiency graph emphasizes how the Nano-Fluid cooling system maintains a stable and higher efficiency profile throughout the day, especially during hours when uncooled systems typically suffer from severe thermal degradation. While both systems follow similar diurnal patterns influenced by solar irradiance, the cooled system consistently outperforms in all parameters due to the enhanced heat dissipation capability of the Nano-Fluid composed of iron particles in coconut oil.

In conclusion, the combined effect of dual-axis solar tracking and Nano-Fluid-based geothermal cooling significantly boosts the PV system's electrical output and efficiency, making it a viable solution for improving the overall performance and reliability of solar energy systems in high-temperature environments.

REFERENCES:

1. J. A. del Cueto, "Closed-form solutions and parameterization of the problem of current–voltage performance of polycrystalline photovoltaic modules deployed at fixed latitude tilt," in Proc. 31st IEEE Photovoltaic Specialists Conf. (PVSC), Lake Buena Vista, FL, Feb. 2005, pp. 1488–1491, doi:10.1109/PVSC.2005.1488136.
2. G. S. Sandhu, M. S. Sodha, and S. I. Anwar, "Experimental investigation of water-cooled photovoltaic panels for enhanced electrical efficiency," Renewable Energy, vol. 102, pp. 336–345, Mar. 2017.

3. S. Riffat and J. Zhu, “Geothermal energy applications: Ground-source heat pumps and ground-coupled heat exchangers,” Int. J. Low-Carbon Technol., vol. 6, no. 3, pp. 153–160, Sep. 2011, doi:10.1093/ijlct/ctr019.
4. M. Akhtar, S. M. Said, and A. H. Al-Mashaqbeh, “Underground heat exchanger cooling for solar panels in arid climates,” Renewable Energy, vol. 76, pp. 536–542, Jun. 2015, doi:10.1016/j.renene.2014.11.020.
5. H. Tyagi, P. Phelan, and R. Prasher, “Predicted efficiency of a low-temperature nanofluid-based direct absorption solar collector,” J. Solar Energy Eng., vol. 131, no. 4, p. 041004, Nov. 2009, doi:10.1115/1.4000121.
6. O. Mahian, F. Saffari, Y. Akhiani, S. Wongwises, and W. Tymchyshyn, “A review of the applications of nanofluids in solar energy," Renew. Sustain. Energy Rev., vol. 24, pp. 418–435, Jun. 2013, doi:10.1016/j.rser.2013.03.044.
7. R. Kalbasi, M. Lakzaei, and H.R. Ghasemi, “Experimental study of Fe_3O_4–oil nanofluid cooling in solar collectors,” Appl. Therm. Eng., vol. 149, pp. 1274–1285, Apr. 2019, doi:10.1016/j.applthermaleng.2018.12.073.
8. A. Pandey, S. Sharma, and R. K. Baredar, “Performance of coconut-oil-based nanofluid in solar thermal applications,” Energy Convers. Manage., vol. 120, pp. 39–47, Nov. 2016, doi:10.1016/j.enconman.2016.04.047.
9. S. Mekhilef, R. Saidur, and A. Safari, “A review on solar energy use in industries,” Renew. Sustain. Energy Rev., vol. 15, no. 4, pp. 1777–1790, May 2011, doi:10.1016/j.rser.2010.11.031.
10. M. T. Chaichan and H. A. Kazem, “Design and control of a dual-axis PV tracking system for desert climates,” Solar Energy, vol. 116, pp. 18–25, Aug. 2015, doi:10.1016/j.solener.2015.04.038.
11. A. Ayyadurai, K. P. Sudheer, and B. S. Kumar, “Performance enhancement of PV module using single-axis tracker and water cooling,” Energy Procedia, vol. 143, pp. 449–456, Oct. 2018, doi:10.1016/j.egypro.2017.12.720.
12. A. Fazlizan, N. F. Saleh, and A. R. Malek, “Performance analysis of air-cooled PVT with ground heat exchanger,” Renewable Energy, vol. 76, pp. 617–627, Jun. 2015, doi:10.1016/j.renene.2014.12.030.
13. A. Bashir and S. Z. Hassan, “Thermoelectric cooling of photovoltaic modules: Experimental study,” Appl. Therm. Eng., vol. 103, pp. 490–501, Aug. 2016, doi:10.1016/j.applthermaleng.2016.04.044.
14. A. Ndiaye, C. Diop, and J.-P. Diagne, “Comparative study of passive cooling for PV systems,” Energy Rep., vol. 6, pp. 532–539, Mar. 2020, doi:10.1016/j.egyr.2020.03.018.
15. H. M. Ali, M. F. Megahed, and O. A. El-Aziz, “Thermal evaluation of nanofluid-cooled PV system,” Thermal Sci., vol. 22, no. 3, pp. 1275–1285, Aug. 2018, doi:10.2298/TSCI161018210A.
16. F. Jahani, M. Saghafi, and A. Kiani, “Performance of Fe_3O_4–oil nanofluid in solar collectors: Experimental investigation,” J. Therm. Anal. Calorim., vol. 144, pp. 1125–1134, Apr. 2021, doi:10.1007/s10973-020-09535-2.
17. D. Kim, Y. Lee, and J. Kim, “Combining solar tracking and active cooling for PV performance enhancement,” Renewable Energy, vol. 150, pp. 659–669, Nov. 2020, doi:10.1016/j.renene.2020.01.102.
18. A. Razali, S. K. Kamaruzzaman, and M. A. Othman, “Underground coil cooling for PV systems,” Energy Build., vol. 198, pp. 150–160, Sep. 2019, doi:10.1016/j.enbuild.2019.06.023.
19. M. Hasanuzzaman, S. Mahbub, and T. Saidur, “Thermal modeling of nanofluid-cooled PV systems,” Renewable Energy, vol. 93, pp. 190–199, Jun. 2016, doi:10.1016/j.renene.2016.02.057.
20. M. H. Khairul, N. Z. Abidin, and C. Y. Leong, “Synergy of tracking and nanofluid cooling in equatorial PV systems,” Energy Convers. Manage., vol. 229, p. 113737, Mar. 2021, doi:10.1016/j.enconman.2020.113737.